Journal of Micromechanics and Molecular Physics
Vol. 1, No. 1 (2016) 1650005 (19 pages)

DOI: 10.1142/S2424913016500053

World Scientific
www.worldscientific.com

An interphase model for effective elastic properties of concrete composites

Chunxiang Shi

College of Urban Construction and Safety Engineering
Shanghai Institute of Technology
Shanghai 201418, P. R. China

Qingsong Tu, Houfu Fan and Shaofan Li*

Department of Civil and Environmental Engineering
University of California, Berkeley, CA 94720, USA

Received February 15, 2016
Accepted March 25, 2016
Published May 3, 2016

Abstract In this work, the Eshelby tensor of a finite spherical domain is employed to construct an interphase model to evaluate elastic properties of concrete composites. Explicit formulations of the interphase model via multi-inclusion method for a class of concrete composites are derived. The theoretical estimate based on an improved Hashin–Shtrikman bounds for the Young's modulus of two-phase concrete composite material are used as a comparison result in the analysis, and the influence of the interfacial transition zone (ITZ) on elastic properties of three-phase concrete composite is studied. Moreover, the homogenization results predicted by the proposed interphase model are compared with the published experimental data. Results obtained in this work show that the proposed interphase model can provide a very accurate estimate of the effective elastic properties of complex concrete composite materials.

Keywords Concrete; composite material; double-inclusion model; Eshelby tensor; homogenization; interphase model.

1. Introduction

Concrete is a complex composite material that consists of multi-scale aggregate particles dispersed in a porous cement paste. Macroscopic mechanical properties and failure mechanism of concrete are determined by the microscopic components. And the interface between aggregate and cement mortar is an important factor that affects the failure path and macro-mechanical properties of concrete. In recent years, concrete has been viewed as a three-phase composite material. By employing the Mori–Tanaka method [Mori and Tanaka, 1973] and the Eshelby equivalent

*Corresponding author. Email: shaofan@berkeley.edu

eigenstrain method [Eshelby, 1957], Yang and Li [Yang and Huang, 1996a,b; Li *et al.*, 1999a,b] estimated the effective elastic constants of concrete materials. The influence of the Young's modulus and volume fraction of each of the three phases: cement paste phase, inter-facial transition zone (ITZ), and the aggregate phase on the effective Young's modulus of the three-phase concrete is well established [Simeonov and Ahmad, 1995; Ramesh *et al.*, 1996; Lutz *et al.*, 1997; Yang, 1998; Sun *et al.*, 2007]. The Hashin–Shtrikman (H–S) bounds [Hashin and Shtrikman, 1963] were also used to assess the significance of transition zone on the overall elastic moduli of cement composites [Nilsen and Monteiro, 1993; Simeonov and Ahmad, 1995].

However, these models are based on classical Eshelby tensors that adopt special assumptions on how the inclusions (aggregate) interact with the matrix (cement paste). For instance, the Mori–Tanaka model assumes a perfect bonding and continuity between the inclusion and matrix. The double-inclusion model developed by Hori and Nemat-Nasser [Hori and Nemat-Nasser, 1994; Nemat-Nasser *et al.*, 1996] is essentially a three-phase composite model consisting of an inclusion embedded in a second inclusion phase, which is further embedded in an infinitely extended (matrix) medium. The double inclusion method may serve as an interphase model. However, if both inclusions are co-axial similar ellipsoids, the interphase effect disappears. In this work, mortar is considered as a composite material in which sand particles are embedded in a matrix of hardened cement paste, and the transition zone is around the sand particles. By employing the finite Eshelby tensors for a spherical inclusion in a finite spherical domain, the double-inclusion theory is extended to a general interphase model that can be used to better approximate the effective elastic properties of concrete composites.

The paper is organized into six sections. In Sec. 2, the concrete composite models are introduced. In Sec. 3, the finite Eshelby tensors for a spherical inclusion in a finite spherical domain are briefly summarized. In Sec. 4, the interphase models via multi-inclusion method, the improved H–S bounds, and their estimates for effective elastic properties of the concrete composite materials are derived. In Sec. 5, a comparison is made between the theoretical results and published experimental data. Finally, in Sec. 6, we close our presentation by making a few remarks.

2. Concrete Composite Model

In this work, a concrete element is considered as a three-phase (mortar, aggregate, and ITZ) composite material, in which the fine aggregate is assumed to be of spherical shape and the ITZ is treated as a uniform layer around the aggregate (shown schematically in Fig. 1). In this way, a concrete is made up of a large number of such basic elements due to aggregate size distributions (shown schematically in Fig. 2). In Fig. 1, r_1 denotes the radius of the aggregate, $r_2 - r_1$ the thickness of ITZ layer, and $r_3 - r_2$ the thickness of mortar layer. E_g, E_i, E_m and v_g, v_i, v_m are

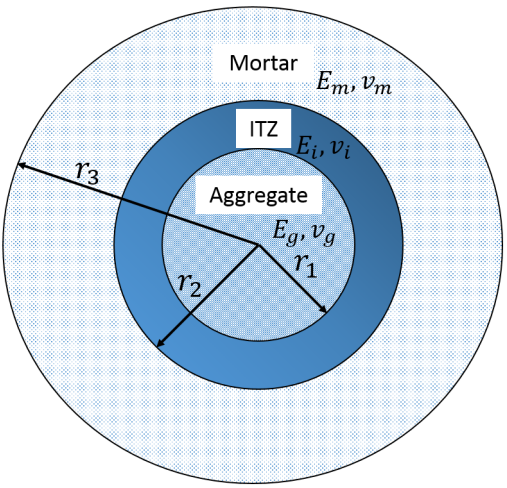

Fig. 1. A basic concrete element.

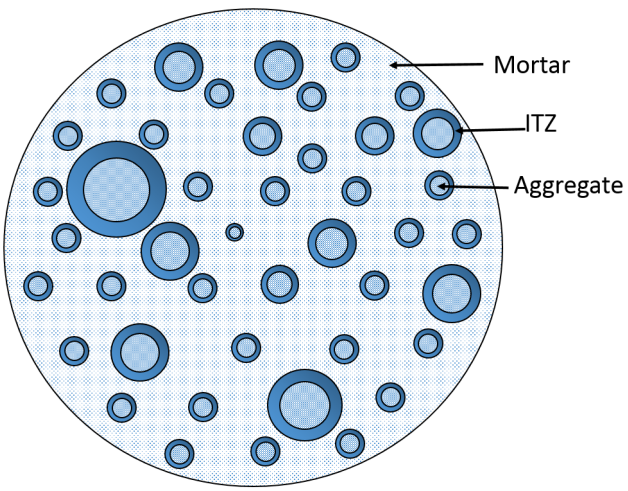

Fig. 2. Concrete composite model.

the Young's modulus and Poisson's ratio of the aggregate, ITZ and mortar. The thickness of the ITZ layer $(r_2 - r_1)$ is assumed to be constant, regardless of the size distribution of aggregates. Based on this assumption, the ITZ layer thickness can be readily estimated [Li *et al.*, 1999a,b].

If the graded aggregates are divided into N grades, the average radius for the ith grade is r_i $(i = 1, 2, 3, \ldots, N)$, and the aggregate volume fraction for ith grade is V_i,

then the total surface area for aggregates in the ith grade is (no summation in i):

$$S_a(i) = \frac{4\pi {r_i}^2}{\frac{4}{3}\pi {r_i}^3} V_i. \tag{2.1}$$

The total surface area for the total N grades can be written as

$$S_a = f_1 \sum_{i=1}^{N} S_a(i), \tag{2.2}$$

where f_1 is the volume fraction of aggregates in concrete. By assuming that every aggregate is coated with the same thickness of ITZ, the ITZ thickness becomes

$$r_2 - r_1 = \frac{f_2}{S_a}, \tag{2.3}$$

where f_2 is the volume fraction of ITZ. Substituting Eqs. (2.1) and (2.2) into Eq. (2.3), the ITZ thickness can be obtained as

$$r_2 - r_1 = \frac{f_2}{3 f_1 \sum_{i=1}^{N} \frac{V_i}{r_i}}, \tag{2.4}$$

then the ITZ volume fraction, f_2, can be derived as

$$f_2 = 3(r_2 - r_1) f_1 \sum_{i=1}^{N} \frac{V_i}{r_i}. \tag{2.5}$$

Obviously, the following relation regarding the composite's volume fractions holds

$$f_1 + f_2 + f_3 = 1, \tag{2.6}$$

in which f_3 is the volume fraction of the mortar.

3. Finite Eshelby Tensors

In this section, the analytical expressions for the Eshelby tensors in finite domains are provided. The exact solutions of the Eshelby tensors for a spherical inclusion in a finite, spherical domain have been obtained for both the Dirichlet and Neumann boundary value problems, and they have been further applied to the homogenization of composites [Li *et al.*, 2007a,b]. In the rest of the paper, we shall call the Eshelby tensors in a finite representative volume element (RVE) as the "Finite Eshelby tensor". Here we consider three materials phases that occupy three non-overlapping domains Ω_1, Ω_2 and Ω_3, where Ω_1 and Ω_2 are assumed to be concentric spherical shells embedded in the matrix Ω_3 (see Fig. 3) with Ω_2 denoting the interphase.

In this three-layer shell model, the RVE consists of three concentric spherical shells, which are labeled as,

$$\begin{aligned} \Omega_1(\mathbf{x}) &= \{\mathbf{x} \,|\, |\mathbf{x}| \le r_1\}, \\ \Omega_2(\mathbf{x}) &= \{\mathbf{x} \,|\, r_1 < |\mathbf{x}| \le r_2\}, \\ \Omega_3(\mathbf{x}) &= \{\mathbf{x} \,|\, r_2 < |\mathbf{x}| \le r_3\}. \end{aligned} \tag{3.1}$$

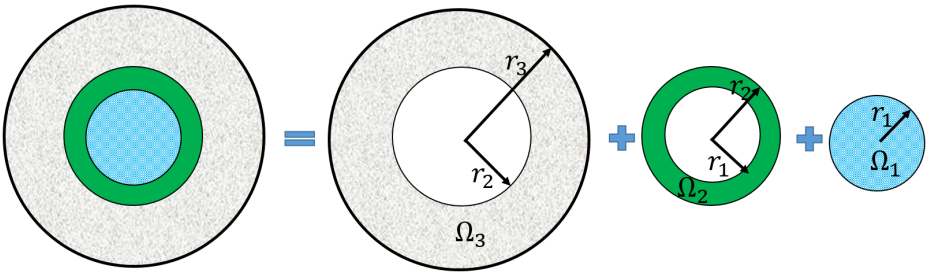

Fig. 3. The three-layer shell model (on the left) is combined by three different shells with different domains and radii.

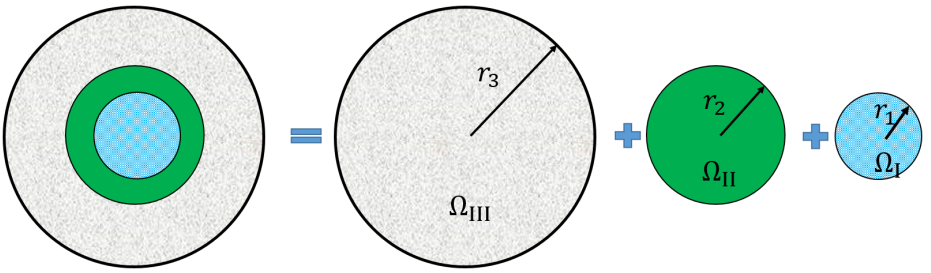

Fig. 4. The three concentric sphere model (on the left) is combined by three different overlapped concentric spheres with different domains and radii.

The radius of the RVE is r_3, and the volume fractions of each phase are as follows,

$$f_1 = \left(\frac{r_1}{r_3}\right)^3, \quad f_2 = \frac{r_2^3 - r_1^3}{r_3^3}, \quad f_3 = \frac{r_3^3 - r_2^3}{r_3^3}. \tag{3.2}$$

Notice that, $f_1 + f_2 + f_3 = 1$.

For the Eshelby tensors of each shell, three partially overlapped concentric spheres are considered, as shown in Fig. 4, with domains defined as

$$\begin{aligned} \Omega_{\mathrm{I}}(\mathbf{x}) &= \{\mathbf{x} \,|\, |\mathbf{x}| \le r_1\}, \\ \Omega_{\mathrm{II}}(\mathbf{x}) &= \{\mathbf{x} \,|\, |\mathbf{x}| \le r_2\}, \\ \Omega_{\mathrm{III}}(\mathbf{x}) &= \{\mathbf{x} \,|\, |\mathbf{x}| \le r_3\}. \end{aligned} \tag{3.3}$$

The interior and exterior Eshelby tensors for each sphere Ω_J are expressed as

$$\mathbb{S}^{J,F}(\mathbf{x}) = \begin{cases} \mathbb{S}^{I,F}(\mathbf{x}), & \forall \mathbf{x} \in \Omega_J, \qquad J = \mathrm{I},\, \mathrm{II},\, \mathrm{III}, \\ \mathbb{S}^{E,F}(\mathbf{x}), & \forall \mathbf{x} \in \Omega/\Omega_J, \quad J = \mathrm{I},\, \mathrm{II},\, \mathrm{III}, \end{cases} \tag{3.4}$$

where the superscript represents the general boundary conditions, and the derivation and expressions for the average Eshelby tensors can be found in Li *et al.* [2007a].

In the subsequent derivation, the average of the Eshelby tensor is needed for each shell. We first denote the average of the Eshelby tensor of the overlapping spheres,

$$\mathbb{S}^{Jj,F} = \langle \mathbb{S}^{J,F} \rangle_{\Omega_j}, \quad J = \text{I, II, III and } j = 1, 2, 3, \tag{3.5}$$

where the first superscript J (Roman numbers) denotes the sphere Ω_J, in which the eigenstrain is prescribed, and the second superscript j (Arabic numbers) denotes the shell Ω_j, over which the average is taken. Similarly the average Eshelby tensors of the three shell domains are represented as

$$\mathbb{S}^{ij,F} = \langle \mathbb{S}^{i,F} \rangle_{\Omega_j}, \quad i = 1, 2, 3, \text{ and } j = 1, 2, 3. \tag{3.6}$$

Again, the first superscript index i refers to the shell region Ω_i, in which the eigenstrains are prescribed, and the second index j denotes the shell Ω_j, over which the average is taken. The average Eshelby tensors can be written as

$$\mathbb{S}^{ij,F} = s_1^{ij,F}\mathbb{E}^{(1)} + s_2^{ij,F}\mathbb{E}^{(2)}, \quad i, j = 1, 2, 3. \tag{3.7}$$

All the coefficients of the Eshelby tensors for each shell layer are expressed in terms of the Eshelby coefficients for solid spheres Ω_{I}, Ω_{II} and Ω_{III}, which are documented in Appendix A for a three-sphere RVE. It has been found that the so-called Dirichlet-SD and Neumann-SN Eshelby tensors are not constant in the interior of the inclusion even for uniformly prescribed eigenstrains. Instead, they are dependent on the position inside the RVE and the volume fraction of the participating phases. It is important to note that in the conventional double inclusion theory the Eshelby tensors used for inclusions are with respect to an infinite matrix, and if the two inclusions are co-axial ellipsoids, the term $\Delta\mathbb{S}_\alpha = \mathbb{S}^{i\alpha} - \mathbb{S}^{p\alpha} = 0$, which means that interphase effect is excluded. However, based on the finite Eshelby tensors, the effect of the term $\Delta\mathbb{S}_\alpha$ is always non-zero, and the interphase effect can be successfully incorporated for a three-phase composite embedded in a finite matrix.

4. Homogenization Model

4.1. *Interphase model based on the multi-inclusion method*

Conventional double-inclusion model, as shown in Fig. 5, is suitable for three-phase concrete composites as proposed in the previous section, and the explicit expressions of effective moduli for composites have been presented [Hori and Nemat-Nasser, 1994; Nemat-Nasser *et al.*, 1996]. Concrete composite material is made up of a large number of concrete elements due to aggregate size distributions, so explicit formulations of the multi-inclusion models for different particle distributions are demanded. In this section, the interphase model is constructed for concrete composite material based on the multi-inclusion method [Lu *et al.*, 2013].

Consider a concrete composite contains N different aggregate distributions. The corresponding interlayer phases, finite volume fractions of mortar (matrix), aggregate (particle), and ITZ (interphase) are defined as f_m, $f_{p\alpha}$ and $f_{i\alpha}$, respectively, which satisfy the relation $f_m + \sum_1^N (f_{p\alpha} + f_{i\alpha}) = 1$ as shown in Fig. 6.

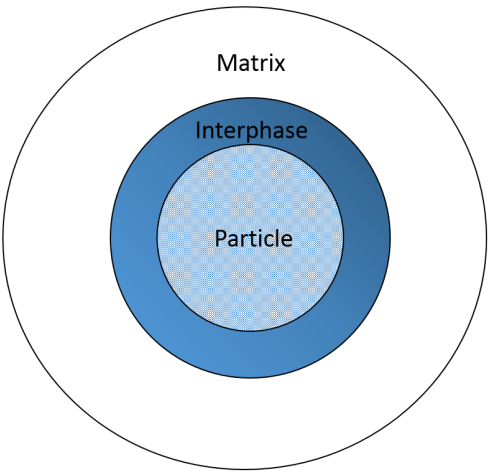

Fig. 5. Double-inclusion model.

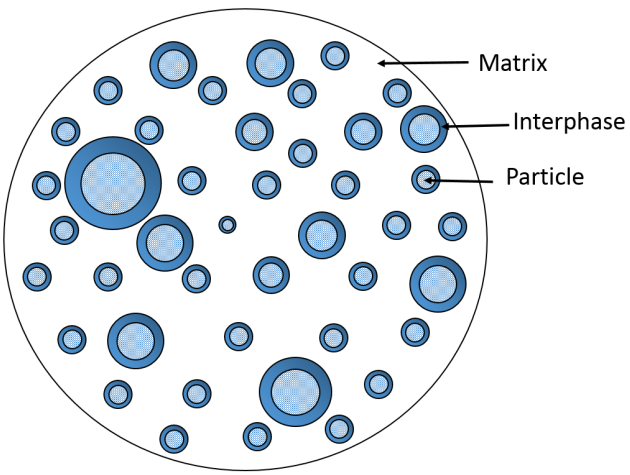

Fig. 6. Multi-inclusion model.

The elastic tensors in the phases are denoted as $\mathbb{C}_m$, $\mathbb{C}_{i\alpha}$ and $\mathbb{C}_{p\alpha}$, with the subscript m, i and p representing the mortar (matrix), ITZ (interphase) and aggregate (particle), respectively. The global strain concentration tensors of the interphase and the particle phase for the αth filler can be obtained as,

$$\mathbb{A}_g^{i\alpha} = \mathbb{A}_{\text{dil}}^{i\alpha} : \left[f_m \mathbb{I} + \sum_{\alpha=1}^{N} \left(f_{i\alpha} \mathbb{A}_{\text{dil}}^{i\alpha} + f_{p\alpha} \mathbb{A}_{\text{dil}}^{p\alpha} \right) \right]^{-1}, \tag{4.1}$$

$$\mathbb{A}_g^{p\alpha} = \mathbb{A}_{\text{dil}}^{p\alpha} : \left[f_m \mathbb{I} + \sum_{\alpha=1}^{N} \left(f_{i\alpha} \mathbb{A}_{\text{dil}}^{i\alpha} + f_{p\alpha} \mathbb{A}_{\text{dil}}^{p\alpha} \right) \right]^{-1}, \tag{4.2}$$

where

$$\mathbb{A}_{\text{dil}}^{i\alpha} = \mathbb{I} + \mathbb{S}^{i\alpha} : \boldsymbol{\Phi}^{i\alpha} + \frac{f_{p\alpha}}{f_{i\alpha}} \Delta\mathbb{S}_\alpha : (\boldsymbol{\Phi}^{p\alpha} - \boldsymbol{\Phi}^{i\alpha}), \tag{4.3}$$

$$\mathbb{A}_{\text{dil}}^{p\alpha} = \mathbb{I} + \mathbb{S}^{p\alpha} : \boldsymbol{\Phi}^{p\alpha} + \Delta\mathbb{S}_\alpha : \boldsymbol{\Phi}^{i\alpha} \tag{4.4}$$

are the dilute strain concentration tensors of the interphase and the particle phases for the αth filler. In the two equations above, $\Delta\mathbb{S}_\alpha = \mathbb{S}^{i\alpha} - \mathbb{S}^{p\alpha}$, $\mathbb{S}^{i\alpha}$ and $\mathbb{S}^{p\alpha}$ are finite Eshelby tensors, which are obtained in Sec. 2, for both the interphase and the particle region corresponding to the αth filler, respectively. $\boldsymbol{\Phi}^{p\alpha}$ and $\boldsymbol{\Phi}^{i\alpha}$ are two fourth-order tensors that are given as follows:

$$\boldsymbol{\Phi}^{p\alpha} = -\Bigg[(\mathbb{S}^{p\alpha} + \mathbb{A}^{p\alpha}) + \Delta\mathbb{S}_\alpha : \left(\mathbb{S}^{p\alpha} + \mathbb{A}^{p\alpha} - \frac{f_{p\alpha}}{f_{i\alpha}}\Delta\mathbb{S}_\alpha\right) : \left(\mathbb{S}^{i\alpha} + \mathbb{A}^{i\alpha} - \frac{f_{i\alpha}}{f_{i\alpha}}\Delta\mathbb{S}_\alpha\right)^{-1}\Bigg]^{-1}, \tag{4.5}$$

$$\boldsymbol{\Phi}^{i\alpha} = -\Bigg[\Delta\mathbb{S}_\alpha + (\mathbb{S}^{p\alpha} + \mathbb{A}^{p\alpha}) : \left(\mathbb{S}^{p\alpha} + \mathbb{A}^{p\alpha} - \frac{f_{p\alpha}}{f_{i\alpha}}\Delta\mathbb{S}_\alpha\right)^{-1} : \left(\mathbb{S}^{i\alpha} + \mathbb{A}^{i\alpha} - \frac{f_{i\alpha}}{f_{i\alpha}}\Delta\mathbb{S}_\alpha\right)\Bigg]^{-1}, \tag{4.6}$$

where $\mathbb{A}^{p\alpha} = (\mathbb{C}^{p\alpha} - \mathbb{C}^m)^{-1} : \mathbb{C}^m$ and $\mathbb{A}^{i\alpha} = (\mathbb{C}^{i\alpha} - \mathbb{C}^m)^{-1} : \mathbb{C}^m$.

The corresponding effective moduli of the multi-inclusion concrete composite are thus given by

$$\bar{\mathbb{C}} = \mathbb{C}^m + \sum_{\alpha=1}^{N} [f_{i\alpha}(\mathbb{C}^{i\alpha} - \mathbb{C}^m) : \mathbb{A}_g^{i\alpha} + f_{p\alpha}(\mathbb{C}^{p\alpha} - \mathbb{C}^m) : \mathbb{A}_g^{p\alpha}]. \tag{4.7}$$

Similarly, the effective moduli of concrete composites with aligned coaxial and similar inclusions can be evaluated as

$$\bar{\mathbb{C}} = \mathbb{C}^m + [f_i(\mathbb{C}^{i\alpha} - \mathbb{C}^m) : \mathbb{A}_g^i + f_p(\mathbb{C}^p - \mathbb{C}^m) : \mathbb{A}_g^p]. \tag{4.8}$$

Using the Voight notation, the elastic tensor of the matrix are

$$\bar{\mathbf{C}} = \begin{bmatrix} \bar{c}_{11} & \bar{c}_{12} & \bar{c}_{13} & 0 & 0 & 0 \\ \bar{c}_{21} & \bar{c}_{22} & \bar{c}_{23} & 0 & 0 & 0 \\ \bar{c}_{31} & \bar{c}_{32} & \bar{c}_{33} & 0 & 0 & 0 \\ 0 & 0 & 0 & \bar{c}_{44} & 0 & 0 \\ 0 & 0 & 0 & 0 & \bar{c}_{55} & 0 \\ 0 & 0 & 0 & 0 & 0 & \bar{c}_{66} \end{bmatrix}. \tag{4.9}$$

For randomly distributed particles, the effective mechanical properties of the composites are isotropic, and there are only two independent effective material

constants. Therefore, the matrix of the effective elastic tensor can be expressed as

$$\bar{\mathbf{C}}_{3D} = \begin{bmatrix} \bar{\bar{\lambda}} + 2\bar{\bar{\mu}} & \bar{\bar{\lambda}} & \bar{\bar{\lambda}} & 0 & 0 & 0 \\ \bar{\bar{\lambda}} & \bar{\bar{\lambda}} + 2\bar{\bar{\mu}} & \bar{\bar{\lambda}} & 0 & 0 & 0 \\ \bar{\bar{\lambda}} & \bar{\bar{\lambda}} & \bar{\bar{\lambda}} + 2\bar{\bar{\mu}} & 0 & 0 & 0 \\ 0 & 0 & 0 & \bar{\bar{\mu}} & 0 & 0 \\ 0 & 0 & 0 & 0 & \bar{\bar{\mu}} & 0 \\ 0 & 0 & 0 & 0 & 0 & \bar{\bar{\mu}} \end{bmatrix}, \tag{4.10}$$

where the effective Lame constants $\bar{\bar{\lambda}}$ and $\bar{\bar{\mu}}$ can be expressed as,

$$\bar{\bar{\lambda}} = \frac{1}{15}(\bar{c}_{11} + 6\bar{c}_{22} + 8\bar{c}_{12} - 10\bar{c}_{44} - 4\bar{c}_{55}), \tag{4.11}$$

$$\bar{\bar{\mu}} = \frac{1}{15}(\bar{c}_{11} + \bar{c}_{22} - 2\bar{c}_{12} + 5\bar{c}_{44} + 6\bar{c}_{55}). \tag{4.12}$$

The effective material constants, such as the effective Young's modulus $\bar{E}$, bulk modulus $\bar{\kappa}$, shear modulus $\bar{\mu}$, Poisson's ratio $\bar{\nu}$, that usually used in engineering applications can be expressed in terms of the effective Lame constants:

$$\bar{E} = \frac{\bar{\bar{\mu}}(3\bar{\bar{\lambda}} + 2\bar{\bar{\mu}})}{\bar{\bar{\lambda}} + \bar{\bar{\mu}}}, \quad \bar{\kappa} = \bar{\bar{\lambda}} + \frac{2}{3}\bar{\bar{\mu}}, \quad \bar{\mu} = \bar{\bar{\mu}}, \quad \bar{\nu} = \frac{\bar{\bar{\lambda}}}{2(\bar{\bar{\lambda}} + \bar{\bar{\mu}})}. \tag{4.13}$$

4.2. *Interphase model via the improved H–S bounds*

In this section, we shall present an interphase model based on the H–S bounds [Hashin and Shtrikman, 1963]. One of the useful homogenization methods for concrete composite materials is the H–S variational bounds, which have been extensively used for estimating effective material properties. In the procedure of deriving the variational bounds, the Eshelby tensor is needed in order to estimate the disturbance strain field due to stress polarization or to estimate the disturbance stress field due to the eigenstrain distributions. Since the classical Eshelby tensor is obtained for an inclusion solution in an unbounded region, in principle, it cannot be directly applied to the derivation of the variational bounds of a composite with finite volume. A modified H–S method that uses the finite Eshelby tensors obtained in Sec. 2, is proposed to improve the conventional H–S bounds. We now consider an isotropic two-phase composite, with $k_2 > k_1$ and $\mu_2 > \mu_1$. For the effective bulk modulus, the following bound under the prescribed displacement boundary condition (Dirichlet-SD) can be obtained as [see: Li *et al.*, 2007a,b]:

$$k_1 + \frac{f_2}{\frac{1}{k_2 - k_1} + \frac{s_1^{22,D}}{k_1}} \leq \bar{k} \leq k_2 + \frac{f_1}{\frac{1}{k_1 - k_2} + \frac{s_1^{11,D}}{k_2}}. \tag{4.14}$$

Similarly, the bounds for the effective shear modulus can be obtained as

$$\mu_1 + \frac{f_2}{\frac{1}{\mu_2-\mu_1} + \frac{s_2^{22,D}}{\mu_1}} \le \bar{\mu} \le \mu_2 + \frac{f_1}{\frac{1}{\mu_1-\mu_2} + \frac{s_2^{11,D}}{\mu_2}}. \tag{4.15}$$

Consider a three-phase isotropic composite denoted by Ω_1, Ω_2 and Ω_3, with Ω_1 denoting the inclusion phase, Ω_2 denoting the interphase, and Ω_3 denoting the matrix. The volume fractions of the matrix, interphase and particle are donted by f_1, f_2, f_3, respectively, which satisfy the relation $f_1 + f_2 + f_3 = 1$. Following the standard procedure of optimization in the H–S bound derivation e.g., Li and Wang [2008], the stationary value of stress polarization in each phase p_i is obtained through the system of equations derived in Li *et al.* [2007b]. To obtain the lower bound, by choosing $k_3 > k_2 > k_1$, $\mu_3 > \mu_2 > \mu_1$, $k_0 = k_1$ and $p_1 = 0$, one can then obtain p_2 and p_3 as follows,

$$p_2 = 3\bar{\epsilon}\underline{p}_2, \quad p_3 = 3\bar{\epsilon}\underline{p}_3, \tag{4.16}$$

$$\underline{p}_2 = \frac{1}{\Delta_{l1}}\left(\frac{s_1^{33,D} - 0.5s_1^{32,D}}{\kappa_1} + \frac{1}{\kappa_3 - \kappa_1}\right), \tag{4.17}$$

$$\underline{p}_3 = \frac{1}{\Delta_{l1}}\left(\frac{s_1^{22,D} - 0.5s_1^{23,D}}{\kappa_1} + \frac{1}{\kappa_2 - \kappa_1}\right), \tag{4.18}$$

where

$$\Delta_{l1} = \left(\frac{s_1^{22,D}}{\kappa_1} + \frac{1}{\kappa_2 - \kappa_1}\right)\left(\frac{s_1^{33,D}}{\kappa_1} + \frac{1}{\kappa_3 - \kappa_1}\right) - \frac{s_1^{32,D}s_1^{23,D}}{4\kappa_1^2}. \tag{4.19}$$

Similarly, one can solve equation for the stationary values of p_1 and p_2 for the upper bound by setting $k_0 = k_3$ and $p_3 = 0$, i.e.,

$$p_1 = 3\bar{\epsilon}\overline{p}_1, \quad p_2 = 3\bar{\epsilon}\overline{p}_2, \tag{4.20}$$

$$\overline{p}_1 = \frac{1}{\Delta_{u1}}\left(\frac{s_1^{22,D} - 0.5s_1^{21,D}}{\kappa_3} + \frac{1}{\kappa_2 - \kappa_3}\right), \tag{4.21}$$

$$\overline{p}_2 = \frac{1}{\Delta_{u1}}\left(\frac{s_1^{11,D} - 0.5s_1^{12,D}}{\kappa_3} + \frac{1}{\kappa_1 - \kappa_3}\right), \tag{4.22}$$

where

$$\Delta_{u1} = \left(\frac{s_1^{11,D}}{\kappa_3} + \frac{1}{\kappa_1 - \kappa_3}\right)\left(\frac{s_1^{22,D}}{\kappa_3} + \frac{1}{\kappa_2 - \kappa_3}\right) - \frac{s_1^{12,D}s_1^{21,D}}{4\kappa_3^2}. \tag{4.23}$$

Substituting the stationary values p_i into the H–S variational inequalities, the explicit variational bounds of the bulk modulus for three-phase composites can

be found as follows,

$$\overline{\kappa} \geq \kappa_1 - \left[\frac{f_2\underline{p}_2^2}{\kappa_2-\kappa_1} + \frac{f_3\underline{p}_3^2}{\kappa_3-\kappa_1}\right] + 2\left(f_2\underline{p}_2 + f_3\underline{p}_3\right) - \frac{1}{\kappa_1}\left(f_2\underline{p}_2^2 s_1^{22,D} + f_2\underline{p}_2\underline{p}_3 s_1^{32,D} + f_3\underline{p}_2\underline{p}_3 s_1^{23,D} + f_3\underline{p}_3^2 s_1^{33,D}\right), \quad (4.24)$$

$$\overline{\kappa} \leq \kappa_3 - \left[\frac{f_1\overline{p}_1^2}{\kappa_1-\kappa_3} + \frac{f_2\overline{p}_2^2}{\kappa_2-\kappa_3}\right] + 2\left(f_1\overline{p}_1 + f_2\overline{p}_2\right) - \frac{1}{\kappa_3}\left(f_1\overline{p}_1^2 s_1^{11,D} + f_1\overline{p}_1\overline{p}_2 s_1^{21,D} + f_2\overline{p}_1\overline{p}_2 s_1^{12,D} + f_2\overline{p}_2^2 s_1^{22,D}\right). \quad (4.25)$$

Similarly, for the variational bounds of the shear modulus we have:

$$\overline{\mu} \geq \mu_1 - \left[\frac{f_2\underline{\tau}_2^2}{\mu_2-\mu_1} + \frac{f_3\underline{\tau}_3^2}{\mu_3-\mu_1}\right] + 2\left(f_2\underline{\tau}_2 + f_3\underline{\tau}_3\right) - \frac{1}{\mu_1}\left(f_2\underline{\tau}_2^2 s_2^{22,D} + f_2\underline{\tau}_2\underline{\tau}_3 s_2^{32,D} + f_3\underline{\tau}_2\underline{\tau}_3 s_2^{23,D} + f_3\underline{\tau}_3^2 s_2^{33,D}\right), \quad (4.26)$$

$$\overline{\mu} \leq \mu_3 - \left[\frac{f_1\overline{\tau}_1^2}{\mu_1-\mu_3} + \frac{f_2\overline{\tau}_2^2}{\mu_2-\mu_3}\right] + 2\left(f_1\overline{\tau}_1 + f_2\overline{\tau}_2\right) - \frac{1}{\mu_3}\left(f_1\overline{\tau}_1^2 s_2^{11,D} + f_1\overline{\tau}_1\overline{\tau}_2 s_2^{21,D} + f_2\overline{\tau}_1\overline{\tau}_2 s_2^{12,D} + f_2\overline{\tau}_2^2 s_2^{22,D}\right), \quad (4.27)$$

where

$$\underline{\tau}_2 = \frac{1}{\Delta_{l2}}\left(\frac{s_2^{33,D} - 0.5 s_2^{32,D}}{\mu_1} + \frac{1}{\mu_3-\mu_1}\right), \quad (4.28)$$

$$\underline{\tau}_3 = \frac{1}{\Delta_{l2}}\left(\frac{s_2^{22,D} - 0.5 s_2^{23,D}}{\mu_1} + \frac{1}{\mu_2-\mu_1}\right), \quad (4.29)$$

$$\overline{\tau}_1 = \frac{1}{\Delta_{u2}}\left(\frac{s_2^{22,D} - 0.5 s_2^{21,D}}{\mu_3} + \frac{1}{\mu_2-\mu_3}\right), \quad (4.30)$$

$$\overline{\tau}_2 = \frac{1}{\Delta_{u2}}\left(\frac{s_2^{11,D} - 0.5 s_2^{12,D}}{\mu_3} + \frac{1}{\mu_1-\mu_3}\right), \quad (4.31)$$

and

$$\Delta_{l2} = \left(\frac{s_2^{22,D}}{\mu_1} + \frac{1}{\mu_2-\mu_1}\right)\left(\frac{s_2^{33,D}}{\mu_1} + \frac{1}{\mu_3-\mu_1}\right) - \frac{s_2^{23,D} s_2^{32,D}}{4\mu_1^2}, \quad (4.32)$$

$$\Delta_{u2} = \left(\frac{s_2^{11,D}}{\mu_3} + \frac{1}{\mu_1-\mu_3}\right)\left(\frac{s_2^{22,D}}{\mu_3} + \frac{1}{\mu_2-\mu_3}\right) - \frac{s_2^{12,D} s_2^{21,D}}{4\mu_3^2}. \quad (4.33)$$

For two-phase and three-phase improved H–S Bounds mentioned above, $s_1^{ij,D}$, $s_2^{ij,D}$, $i, j = 1, 2, 3$ can be found in Appendix A. The effective Young's modulus can be obtained as

$$\bar{E} = \frac{9\bar{k}\bar{\mu}}{3\bar{k} + \bar{\mu}}. \tag{4.34}$$

5. Results and Discussions

In this section, numerical results are presented to verify the proposed interphase model and to study the ITZ effect on the effective properties of concrete. In the calculations, experimental data [Anson and Newman, 1966] for the Young's modulus and Poisson's ratio of mortar and concrete with different aggregate volume fractions are used as the benchmark example. The experimental data for mortar with water/cement ratio $w/c = 0.5$, $E_m = 28.3\,\text{GPa}$, $\nu_m = 0.171$ and for gravel with $E_g = 69\,\text{GPa}$, $\nu_g = 0.14$ are selected to compare with the theoretical results. The volume fraction of aggregate varies from 0.18 to 0.40.

5.1. *Two-phase model results comparison with experimental data*

Here, the concrete is considered as a two-phase composite without considering ITZ effect. The overall Young's modulus and Poisson's ratio of the two-phase concrete are calculated from Eq. (4.13). Table 1 lists the average theoretical results, experimental data and the improved two-phase model H–S bounds are calculated from Eqs. (4.14), (4.15) and (4.34). It can be seen that the theoretical improved H–S bounds can characterize the main trend of the experimental data for a two-phase composite. But most of the calculated Young's modulus are higher than the experimental results (see Table 1). Thus, it might be necessary to consider the influence of ITZ on the Young's modulus of concrete, and further study is needed.

5.2. *Three-phase model results comparison with experimental data*

In this section, we consider the concrete as a three phase composite with the ITZ effect. The influence of ITZ on the elastic properties of concrete depends mainly on the volume fraction and modulus of elasticity of ITZ. It is found that the average thickness of ITZ layer in typical concrete material is about 0.05 mm [Li *et al.*, 1999a,b]. Assuming that the term $r_2 - r_1$ in Eq. (2.4) is about 0.05 mm, and the ITZ volume fraction, f_2, can be derived as

$$f_2 = 0.15 f_1 \sum_{i=1}^{N} \frac{V_i}{r_i}. \tag{5.1}$$

According to Lutz *et al.* [1997], the elastic modulus of ITZ is about 40% of the elastic modulus of mortar, so that the Young's modulus of ITZ in phase 2 is

Table 1. The calculated results (two-phase model) and experimental data of concrete.

Mortar $E_m = 28.3$ Gpa $v_m = 0.171$	Gravel $E_g = 69$ Gpa $v_g = 0.14$	Concrete E_c (Gpa) (Measured)	Concrete E_c (Gpa) (Calculated)	IMP-HS bounds E (Gpa)		Poisson's ratio V_c (Measured)	Poisson's ratio v (Calculated)
f_3	f_1			Lower	Upper		
0.82	0.18	34.90	33.38	33.02	33.89	0.172	0.165
0.75	0.25	34.20	35.76	35.10	36.27	0.152	0.163
0.72	0.28	35.4	36.84	36.04	37.32	0.160	0.161
0.70	0.30	36.2	37.59	36.68	38.04	0.156	0.160
0.65	0.35	38.6	39.89	38.33	39.86	0.145	0.159
0.60	0.40	39.6	41.54	40.06	41.73	0.153	0.157

Table 2. The calculated results (three-phase model) and experimental data of concrete.

Mortar $E_m = 28.3$ Gpa $v_m = 0.171$	ITZ $E_i = 0.4E_m$ $v_i = 0.171$	Gravel $E_g = 69$ Gpa $v_g = 0.14$	Concrete[a] E_c (Gpa) (Measured)	Concrete E (Gpa) (Calculated)	IMP-HS bounds E (Gpa)		Poisson's ratio V_c ratio v_c (Measured)	Poisson's ratio v (Calculated)
f_3	f_2	f_1			Lower	Upper		
0.782	0.038	0.18	34.90	32.44	31.93	33.06	0.172	0.165
0.698	0.052	0.25	34.20	34.45	33.50	35.03	0.152	0.162
0.661	0.059	0.28	35.40	35.37	34.20	35.91	0.160	0.161
0.637	0.063	0.30	36.20	36.01	34.67	36.50	0.156	0.160
0.577	0.073	0.35	38.60	37.67	35.90	38.00	0.145	0.158
0.516	0.084	0.40	39.60	39.43	37.17	39.55	0.153	0.156

[a]Anson and Newman (1966).

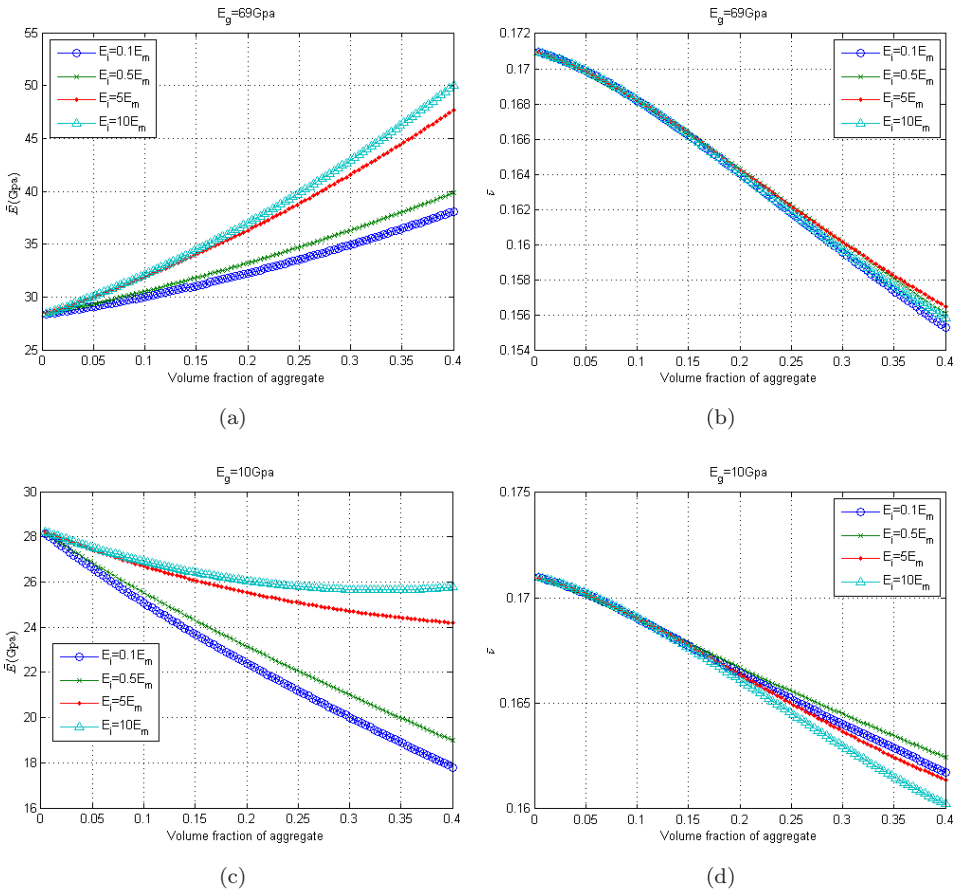

Fig. 7. Effective material properties of the concrete as a function of the aggregate volume with different E_i/E_m.

$E_i = 0.4E_m$. The Poisson's ratio of ITZ ν_i is 0.171, same as that of the mortar phase. The overall elastic Young's modulus and Poisson's ratio of the three-phase concrete are also calculated from Eq. (4.13). Table 2 displays the average theoretical results, experimental data and the improved three-phase model H–S bounds calculated from Eqs. (4.24) through (4.27) and (4.34). It can be seen that for different fractions of different phases, both the Young's modulus and the Poisson's ratio obtained from the three-phase model are very close to that of the experiment results. In addition, the mix proportions have only a little effect on Poisson's ratio. These results suggest that the proposed interphase models can be used to estimate the effective elastic modulus of concrete.

Figures 7 and 8 show the effect of ITZ/mortar Young's modulus ratio ($E_i/E_m = 10, 5, 0.5, 0.1$) and ITZ thickness ($r_2 - r_1 = 0.01, 0.05, 0.07, 0.09$ mm) on the effective Young's modulus and effective Poisson's ratio of concrete with respect to the

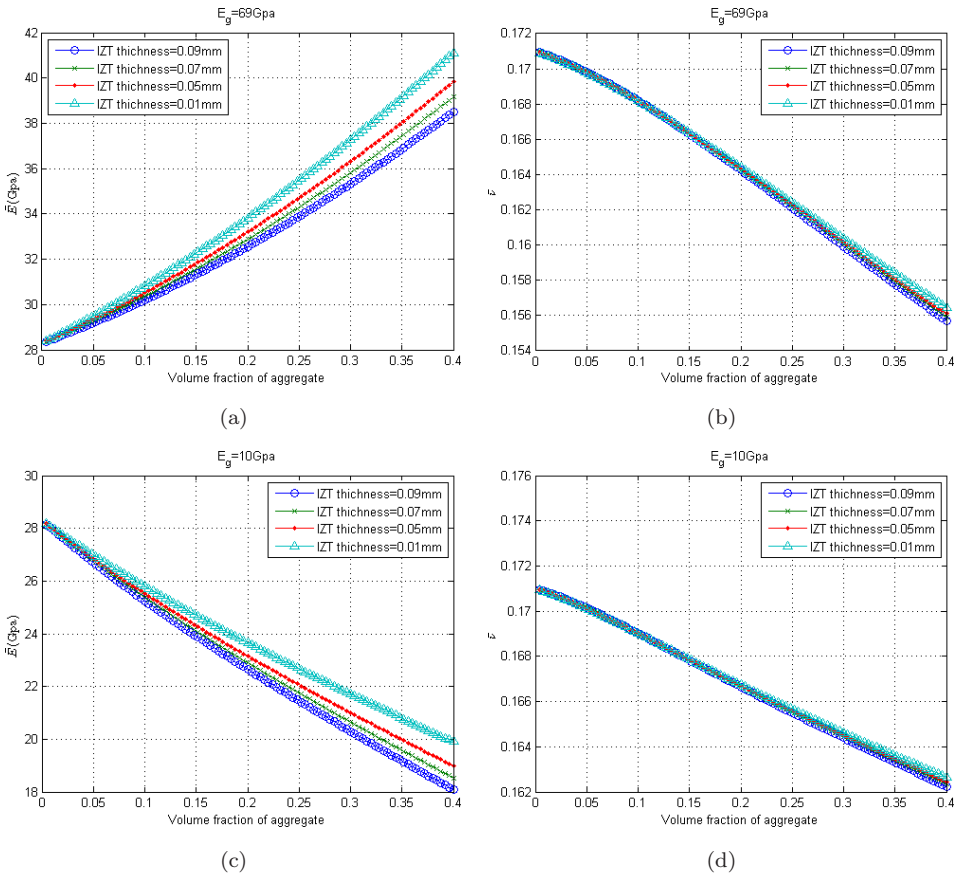

Fig. 8. Effective material properties of the concrete as a function of the aggregate volume with different ITZ thicknesses.

volume fraction of the aggregate. Two types of aggregates are considered: One is a common aggregate with $E_g = 69\,\text{GPa}$, and the other is a lightweight aggregate with $E_g = 10\,\text{GPa}$. For concrete composed of common aggregates, the effective Young's modulus of the concrete increases as the volume fraction of the aggregate increases. For concrete composed of lightweight aggregates, the effective Young's modulus of the concrete decreases as the volume fraction of the aggregate increases, thus the effect of the aggregate concentration on elastic modulus is opposite to common belief. This result indicates that using a densely graded aggregate is an efficient way of increasing the effective Young's modulus of concrete.

Figure 7 shows that for $E_i/E_m > 1$, i.e., the ITZ is harder than the mortar, and the effective Young's modulus of concrete are higher than that for $E_i/E_m < 1$. This result indicates that strengthening the bonding between mortar and aggregate, i.e., increasing the Young's modulus of ITZ(E_i) is very effective for enhancing the effective Young's modulus of concrete materials. In addition, the theoretical

estimate of Poisson's ratio is very insensitive to the ITZ/mortar Young's modulus ratio.

Figure 8 shows that the effective Young's modulus of the concrete increases as the ITZ thickness decreases. This result indicates that decreasing the water/cement ratio or incorporating silica fume are efficient ways of increasing the effective Young's modulus of concrete. In addition, the theoretical estimate of Poisson's ratio is also very insensitive to the ITZ thickness.

6. Conclusions

Concrete is a composite material that is made up of a large number of inhomogeneous elements due to aggregate distributions. In this work, by considering a basic concrete element as a three-phase (mortar, aggregate, and ITZ). To evaluate elastic properties of concrete composites, the finite Eshelby tensors for a spherical inclusion in a finite spherical domain are employed to construct the interphase models, and the explicit formulations of the interphase models via multi-inclusion method for concrete composites are derived. Different estimations for effective mechanical properties of the concrete composite materials are presented. To improve the conventional H–S method, a modified H–S model is given as a function of properties and volume fraction of the composite materials. The effective material properties predicted by the interphase models are compared with the experimental results [Anson and Newman, 1966]. First, the concrete is modeled as a two-phase composite without any ITZ effect, the results show that the experimental data follow the main trend of the theoretical estimate of the improved H–S bounds for a two-phase composite, but most of the measured Young's moduli stay below the calculated results. Then the influence of ITZ on the Young's modulus of concrete is considered, and the concrete is modeled as a three-phase composite with the ITZ effect. A reasonable agreement is found between the theoretical predictions and the experimental results. These results suggest that the proposed interphase models can be used to estimate the effective elastic modulus of concrete.

Acknowledgments

Shi is supported by a fellowship from the Faculty Training Project by Shanghai City Municipal Education Commission, and Tu and Fan are partially supported by a fellowship from Chinese Scholar Council (CSC). Their supports are gratefully acknowledged.

References

Anson, M. and Newman, K. [1966] "The effect of mix proportions and method of testing on Poisson's ratio for mortars and concretes," *Magazine of Concrete Research* **18**(56), 115–130.

Eshelby, J. D. [1957] "The determination of the elastic field of an ellipsoidal inclusion, and related problems," *Proceedings of the Royal Society A* **241**, 376–396.

Hashin, Z. and Shtrikman, S. [1963] "A variational approach to the theory of the elastic behavior of multuphase materials," *Journal of the Mechanics and Physics of Solids* **11**(42), 127–140.

Hori, M. and Nemat-Nasser, S. [1994] "Double-inclusion model and overall moduli of multi-phase composites," *Journal of Engineering Materials and Technology* **116**, 305.

Li, S., Sauer, R. A. and Wang, G. [2007a] "The Eshelby tensors in a finite spherical domain. Part I: Theoretical formulations," *Journal of Applied Mechanics* **74**(4), 770–783.

Li, S. and Wang, G. [2008] *Introduction to Micromechanics and Nanomechanics* (World Scientific Pub., New Jersey).

Li, S., Wang, G. and Sauer, R. A. [2007b] "The Eshelby tensors in a finite spherical domain. Part II: Applications to Homogenization," *Journal of Applied Mechanics* **74**(4), 784–797.

Li, G., Zhao, Y. and Pang, S.-S. [1999a] "Four-phase sphere modeling of effective bulk modulus of concrete," *Cement and Concrete Research* **29**(6), 839–845.

Li, G., Zhao, Y., Pang, S.-S. and Li, Y. [1999b] "Effective Young's modulus estimation of concrete," *Cement and Concrete Research* **29**(9), 1455–1462.

Lu, P., Leong, Y. W., Pallathadka, P. K. and He, C. B. [2013] "Effective moduli of nanoparticle reinforced composites considering interphase effect by extended double-inclusion model — theory and explicit expressions," *International Journal of Engineering Science* **73**, 33–55.

Lutz, M., Monteiro, P. and Zimmermanz, R. [1997] "Inhomogeneous interfacial transition zone model for the bulk modulus of mortar," *Cement and Concrete Research* **27**(1), 1113–1122.

Mori, T. and Tanaka, K. [1973] "Average stress in matrix and average elastic energy of materials with misfitting inclusions," *Acta Metallurgica* **21**, 571–574.

Nemat-Nasser, S., Lori, M. and Datta, S. K. [1996] "Micromechanics: Overall properties of heterogeneous materials," *Journal of Applied Mechanics* **63**, 561.

Nilsen, A. and Monteiro, P. [1993] "Concrete: A three-phase material," *Cement and Concrete Research* **23**(4), 147–151.

Ramesh, G., Sotelino, E. D. and Chen, W. F. [1996] "Effect of transition zone on elastic moduli of concrete materials," *Cement and Concrete Research* **26**(4), 611–622.

Simeonov, P. and Ahmad, S. [1995] "Effect of transition zone on the elastic behavior of cement-based composites," *Cement and Concrete Research* **25**(1), 165–176.

Sun, Z., Garboczi, E. J. and Shah, S. P. [2007] "Modeling the elastic properties of concrete composites: Experiment, differential effective medium theory, and numerical simulation," *Cement and Concrete Composites* **29**(1), 22–38.

Yang, C. C. [1998] "Effect of the transition zone on the elastic moduli of mortar," *Cement and Concrete Research* **28**(5), 727–736.

Yang, C. C. and Huang, R. [1996a] "Double inclusion model for approximate elastic moduli of concrete material," *Cement and Concrete Research* **26**(1), 83–91.

Yang, C. C. and Huang, R. [1996b] "A two-phase model for predicting the compressive strength of concrete," *Cement and Concrete Research* **26**(10), 1567–1577.

Appendix A: Table of Coefficients of Eshelby Tensors for a Three-Layer Spherical RVE

In this Appendix, we provide a complete list of the coefficients for the average Eshelby tensors of a three-sphere phase RVE.

$$s_1^{\mathrm{I1},D} = \frac{(1+\nu)(1-f_1)}{3(1-\nu)},$$

$$s_1^{\mathrm{I1},N} = \frac{(1+\nu)+2(1-2\nu)f_1}{3(1-\nu)},$$

$$s_2^{\mathrm{I1},D} = \frac{2(4-5\nu)(1-f_1)}{15(1-\nu)} - 21\gamma_u[f_1](1-f_1^{2/3}),$$

$$s_2^{\mathrm{I1},N} = \frac{2(4-5\nu)(1-f_1)+(7-5\nu)f_1}{15(1-\nu)} - 21\gamma_t[f_1](1-f_1^{2/3}),$$

$$s_1^{\mathrm{I2},D} = -\frac{(1+\nu)(1-f_1)}{3(1-\nu)},$$

$$s_1^{\mathrm{I2},N} = \frac{2(1-2\nu)f_1}{3(1-\nu)},$$

$$s_2^{\mathrm{I2},D} = -\frac{2(4-5\nu)(1-f_1)}{15(1-\nu)} + 21\gamma_u[f_1]\left(1-\frac{(f_1+f_2)^{5/3}-f_1^{5/3}}{f_2}\right),$$

$$s_2^{\mathrm{I2},N} = \frac{(7-5\nu)f_1}{15(1-\nu)} + 21\gamma_t[f_1]\left(1-\frac{(f_1+f_2)^{5/3}-f_1^{5/3}}{f_2}\right),$$

$$s_1^{\mathrm{I3},D} = -\frac{(1+\nu)(1-f_1)}{3(1-\nu)},$$

$$s_1^{\mathrm{I3},N} = \frac{2(1-2\nu)f_1}{3(1-\nu)},$$

$$s_2^{\mathrm{I3},D} = -\frac{2(4-5\nu)f_1}{15(1-\nu)} + 21\gamma_u[f_1]\left(\frac{(f_1+f_2)(1-(f_1+f_2)^{2/3})}{f_3}\right),$$

$$s_2^{\mathrm{I3},N} = \frac{(7-5\nu)f_1}{15(1-\nu)} - 21\gamma_t[f_1]\frac{(f_1+f_2)\left(1-(f_1+f_2)^{2/3}\right)}{f_3},$$

$$s_1^{\mathrm{II1},D} = \frac{(1+\nu)f_3}{3(1-\nu)},$$

$$s_1^{\mathrm{II1},N} = \frac{(1+\nu)+2(1-2\nu)(f_1+f_2)}{3(1-\nu)},$$

$$s_2^{\mathrm{II1},D} = \frac{2(4-5\nu)f_3}{15(1-\nu)} - 21\gamma_u[f_1]\,(f_1+f_2)\,(1-f_1^{2/3}),$$

$$s_2^{\mathrm{II}1,N} = \frac{2(4-5\nu)+(7-5\nu)(f_1+f_2)}{15(1-\nu)} + 21\gamma_t[f_1+f_2](1-f_1^{2/3}),$$

$$s_1^{\mathrm{II}2,D} = \frac{(1+\nu)f_3}{3(1-\nu)},$$

$$s_1^{\mathrm{II}2,N} = \frac{(1+\nu)2(1-2\nu)(f_1+f_2)}{3(1-\nu)},$$

$$s_2^{\mathrm{II}2,D} = \frac{2(4-5\nu)f_3}{15(1-\nu)} - 21\gamma_u[f_1+f_2]\left(1-\frac{(f_1+f_2)^{5/3}-f_1^{5/3}}{f_2}\right),$$

$$s_2^{\mathrm{II}2,N} = \frac{2(4-5\nu)+(7-5\nu)(f_1+f_2)}{15(1-\nu)} + 21\gamma_t[f_1+f_2]\left(1-\frac{(f_1+f_2)^{5/3}-f_1^{5/3}}{f_2}\right),$$

$$s_1^{\mathrm{II}3,D} = -\frac{(1+\nu)(f_1+f_2)}{3(1-\nu)},$$

$$s_1^{\mathrm{II}2,N} = \frac{2(1-2\nu)(f_1+f_2)}{3(1-\nu)},$$

$$s_2^{\mathrm{II}3,D} = -\frac{2(4-5\nu)(f_1+f_2)}{15(1-\nu)} + 21\gamma_u[f_1+f_2]\left(\frac{(f_1+f_2)(1-(f_1+f_2)^{2/3})}{f_3}\right),$$

$$s_2^{\mathrm{II}3,N} = \frac{(7-5\nu)(f_1+f_2)}{15(1-\nu)} - 21\gamma_t[f_1]\frac{(f_1+f_2)\big(1-(f_1+f_2)^{2/3}\big)}{f_3},$$

$$s_1^{\mathrm{III}3,D} = 0, \quad s_1^{\mathrm{III}3,N} = 1,$$

$$s_2^{\mathrm{III}3,D} = 0, \quad s_2^{\mathrm{III}3,N} = 1,$$

$$s_1^{\mathrm{III}1,D} = 0, \quad s_1^{\mathrm{III}1,N} = 1,$$

$$s_2^{\mathrm{III}1,D} = 0, \quad s_2^{\mathrm{III}1,N} = 1,$$

$$s_1^{\mathrm{III}2,D} = 0, \quad s_1^{\mathrm{III}2,N} = 1,$$

$$s_2^{\mathrm{III}2,D} = 0, \quad s_2^{\mathrm{III}2,N} = 1,$$

where

$$\gamma_u[x] = \frac{x(1-x^{2/3})}{10(1-\nu)(7-10\nu)},$$

$$\gamma_t[x] = \frac{4x(1-x^{2/3})}{10(1-\nu)(7+5\nu)},$$

where the superscript D indicates that the RVE is subjected to the Dirichlet boundary condition or displacement boundary condition; whereas the superscript N indicates that the RVE is subjected to the Neumann boundary condition, or the traction boundary condition. The superscripts with the roman numericals I, II and III indicate the different phases I, II and III.